Ultimate Regime of High Rayleigh Number Convection in a Porous Medium

Duncan R. Hewitt,[1] Jerome A. Neufeld,[1,2,3] and John R. Lister[1]

[1]*Institute of Theoretical Geophysics, DAMTP, University of Cambridge, Wilberforce Road, Cambridge, CB3 0WA, United Kingdom*
[2]*Department of Earth Sciences, University of Cambridge, Cambridge, United Kingdom*
[3]*BP Institute, University of Cambridge, Cambridge, United Kingdom*

(Received 8 February 2012; published 30 May 2012)

Well-resolved direct numerical simulations of 2D Rayleigh-Bénard convection in a porous medium are presented for Rayleigh numbers $\mathrm{Ra} \leq 4 \times 10^4$ which reveal that, contrary to previous indications, the linear classical scaling for the Nusselt number, $\mathrm{Nu} \sim \mathrm{Ra}$, is attained asymptotically. The flow dynamics are analyzed, and the interior of the vigorously convecting system is shown to be increasingly well described as $\mathrm{Ra} \to \infty$ by a simple columnar "heat-exchanger" model with a single horizontal wave number k and a linear background temperature field. The numerical results are approximately fitted by $k \sim \mathrm{Ra}^{0.4}$.

DOI: 10.1103/PhysRevLett.108.224503 PACS numbers: 47.56.+r, 44.30.+v, 47.55.P−

The buoyancy-driven convection of a layer of Boussinesq fluid in a Rayleigh-Bénard cell is a canonical physical system for the study of nonlinear chaotic dynamics and emergent patterns [1,2]. Characterization of the physical control and parameter dependence of the convective buoyancy flux in such a system, as measured by the Nusselt number Nu, is of direct applicability to an extremely wide range of convective flows in environmental and industrial settings. In particular, the dependence of Nu on the Rayleigh number, which is the ratio of driving buoyancy forces to the dissipative effects of viscosity and diffusion, remains an enduring and active subject of fundamental interest in fluid dynamics [3–5].

The related problem of two-dimensional Rayleigh-Bénard convection in a fluid-saturated porous medium has received relatively little attention until recently, particularly at very large values of Ra. There is emerging interest in this subject due to its important implications for the long-term storage of CO_2 in deep saline aquifers [6], which is being widely considered as a means of offsetting anthropogenic emissions of CO_2 and mitigating the effects of climate change [7]. For $\mathrm{Ra} > \mathrm{Ra}_c = 4\pi^2$ the system is unstable to large-scale convective rolls [8]. As Ra is increased, these convective rolls undergo a series of "dripping" instabilities that perturb, but do not significantly alter, the large-scale background flow [9]. For $\mathrm{Ra} \gtrsim 1300$ this quasisteady background flow breaks down completely [10], marking a transition to the "turbulent" high-Ra regime of interest here.

The "classical" argument [11] for the dependence Nu (Ra) suggests that, at sufficiently large values of Ra, the buoyancy flux should be independent of the height H of the layer. For the high-Ra regime in a porous medium this argument predicts a linear scaling $\mathrm{Nu} \sim \mathrm{Ra}$. A linear scaling has also been shown to be a rigorous upper bound [10,12,13]. The high-Ra scaling has been investigated numerically by Otero *et al.* [10] who found a reduced exponent $\mathrm{Nu} \sim \mathrm{Ra}^{0.9}$ for $1300 \lesssim \mathrm{Ra} \lesssim 10\,000$. Experimental results from a one-sided system with a convecting upper boundary and a deep or no-flux bottom boundary have given scalings closer to $\mathrm{Nu} \sim \mathrm{Ra}^{0.8}$ [14,15].

Here we consider a fluid-saturated two-dimensional porous medium with constant permeability Π and porosity ϕ. The domain is heated at the base and cooled at the top, and the fluid satisfies a linear equation of state such that the resulting density difference $\Delta\rho$ across the height of the domain is unstable. The flow is incompressible and governed by Darcy's law. We assume that there is negligible heat transfer to the solid phase of the medium, and employ a constant thermal diffusivity D. This system is therefore analogous to purely compositionally-driven convection.

We introduce a stream function ψ to describe the fluid velocity $(u, w) = (\psi_z, -\psi_x)$, and nondimensionalize with respect to the height of the domain H and the convective velocity scale $U = \Pi g \Delta\rho/\mu$, where μ is the viscosity of the fluid, thus obtaining dimensionless equations

$$\nabla^2 \psi = -\frac{\partial T}{\partial x}, \tag{1}$$

$$\frac{\partial T}{\partial t} + \frac{\partial \psi}{\partial z}\frac{\partial T}{\partial x} - \frac{\partial \psi}{\partial x}\frac{\partial T}{\partial z} = \frac{1}{\mathrm{Ra}}\nabla^2 T. \tag{2}$$

The Rayleigh number Ra is defined as $\mathrm{Ra} \equiv UH/\phi D$. The dimensionless buoyancy flux is given by the Nusselt number $\mathrm{Nu} = \langle L^{-1} \int \partial T/\partial z|_{z=0} dx \rangle$, where L is the dimensionless aspect ratio and $\langle\,\rangle$ denotes a time average. Nondimensionalizing in this way gives rise to $O(1)$ height, temperature, velocity, and convective time scales, while diffusive time and length scales are $O(\mathrm{Ra}^{-1})$.

Equations (1) and (2), are solved numerically, using a spectral method for (1) and an alternating-direction implicit method for (2). The diffusion and advection operators in (2) are discretized using standard second-order finite differences and flux-conservative techniques, respectively.

We use a vertical coordinate transformation in order to resolve the diffusive boundary layers at $z = 0$, 1 which have an anticipated depth $\delta \sim \mathrm{Ra}^{-1}$ [16]. The numerical simulations are second order in space and time, and have been extensively benchmarked against previous numerical results at lower values of Ra [9,10].

For $\mathrm{Ra} \gtrsim 1300$ [17] the system cannot sustain the large-scale quasiperiodic roll structure found at lower Ra, which is broken down as unsteady plumes from the boundaries drive vigorous columnar exchange flow across the height of the domain. This transition in the dynamics marks the start of the "high-Ra" regime. The flow can be divided into three regions of differing dynamics, as illustrated in Fig. 1. The interior region is dominated by predominantly vertical exchange flow, carried in columns or "megaplumes" of a fairly regular and Ra-dependent wavelength. At the very top and bottom of the domain are thin diffusive boundary layers, where intermittent short-wavelength instabilities drive the growth of small "protoplumes." Between the boundary layers and the interior columnar flow is a region where the dynamics are characterized by the rapid growth and vigorous mixing of protoplumes. Lateral flushing by the large-scale flow drives entrainment of the protoplumes into the interior megaplumes.

In the high-Ra regime the local time-dependent Nusselt number exhibits chaotic fluctuations about the long-term time-averaged Nusselt number Nu. A numerical estimate of Nu is obtained by time averaging until statistical uncertainty in the mean is reduced to within 1%. Figure 2 shows Nu(Ra) for $\mathrm{Ra} \leq 40\,000$. The transition to the high-Ra regime is marked by a sharp discontinuity in Nu at $\mathrm{Ra} \approx 1300$; a least-squares fit of the data beyond this point gives a scaling of $\mathrm{Ra} \sim \mathrm{Nu}^{0.95\pm0.01}$, in approximate agreement with previous results [10]. However, the inset to Fig. 2 shows a clear trend in Nu/Ra towards a constant as Ra increases beyond 10 000, strongly suggesting that the classical linear scaling is attained asymptotically. Given that the system is dominated by persistent columnar exchange flow across the whole domain (Fig. 1), it is surprising that the flux seems to be asymptotically independent of the height of the domain. We find that Nu exhibits no systematic dependence on the aspect ratio L; the slight scatter in the measurements of Fig. 2 (inset) is the result of extremely long-time-scale fluctuations in the number of megaplumes in the domain.

We can model the interior megaplume flow by an exact "heat-exchanger" solution to (1) and (2) in an unbounded domain. In this model, vertical advection of a background linear temperature gradient is exactly balanced by horizontal diffusion between neighboring megaplumes, giving a steady solution

$$T(x, z) = \hat{T}\cos(kx) - \frac{k^2}{\mathrm{Ra}}z, \tag{3}$$

$$u = 0, \qquad w(x) = \hat{T}\cos(kx). \tag{4}$$

This solution comprises interlocking columnar flow with amplitude $\hat{T}$ and a regular horizontal wave number k.

Equation (3) shows that the horizontally averaged temperature profile is linear. Numerical measurements of the temporally and horizontally averaged temperature $\langle \bar{T}(z) \rangle$ [Fig. 3(a)] agree with this linear behavior in the interior region. We compare the amplitude of the columnar flow in the model with the numerical calculations by measuring the root-mean-square (rms) temperature perturbations and velocity components, T_{rms}, u_{rms}, and w_{rms}. In the heat-exchanger model, $T_{\mathrm{rms}} = w_{\mathrm{rms}} = \hat{T}/\sqrt{2}$, and $u_{\mathrm{rms}} = 0$. Numerical measurements of T_{rms}, u_{rms}, and w_{rms} at $z = 0.5$ [Fig. 3(b)] show very good agreement with this behavior asymptotically.

These measurements, together with movies [18] of the temperature field, indicate that the vigorously convecting system is dominated by remarkably persistent columnar flow, which becomes increasingly ordered and increasingly well-described by the steady heat-exchanger solution as Ra increases. Moreover, Fig. 3(b) suggests that $\hat{T}$ is asymptotically independent of Ra. This observation agrees with the indications in Fig. 2 that a linear scaling for Nu(Ra) is attained asymptotically: since the heat transport is dominated by advection in the interior, we expect that $\mathrm{Nu} \sim \mathrm{Ra}(T - \bar{T})w \sim \mathrm{Ra}\hat{T}^2 \sim \mathrm{Ra}$, if $\hat{T} = O(1)$.

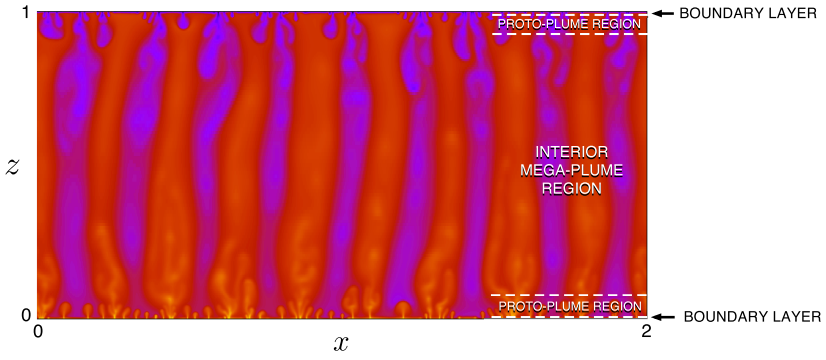

FIG. 1 (color online). A snapshot of the temperature field at $\mathrm{Ra} = 2 \times 10^4$, illustrating the different regions described in the text.

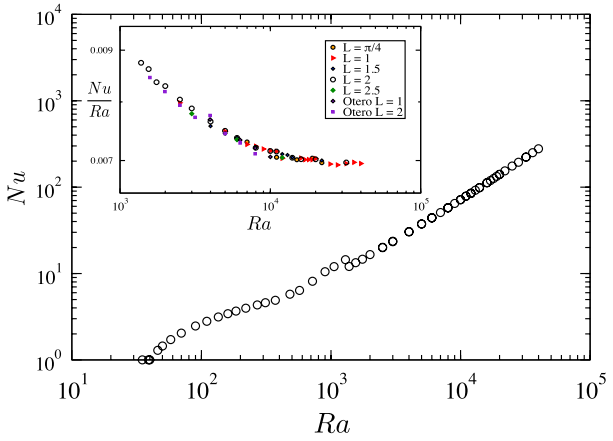

FIG. 2 (color online). The time-averaged Nusselt number Nu, showing the onset of convection at $\mathrm{Ra} = 4\pi^2$, and the transition to the high-Ra regime at $\mathrm{Ra} \approx 1300$. Inset: Nu scaled by Ra in the high-Ra regime, for different aspect ratios L, together with the highest data from [10] for comparison. This plot shows a clear trend in Nu/Ra towards a constant as Ra increases.

We have adapted the unbounded heat-exchanger solution to model the effect of circulation in a finite domain, by including vertical variation with wave number m. We expect that m is related to the height of the domain, which implies that the more rapid horizontal variations with wave number k dominate as Ra increases; hence the simple heat-exchanger solution (3) and (4), is recovered asymptotically. Predictions from the adapted model (not included here) show a good quantitative agreement with the behavior of the rms temperature and velocity perturbations in Fig. 3(b).

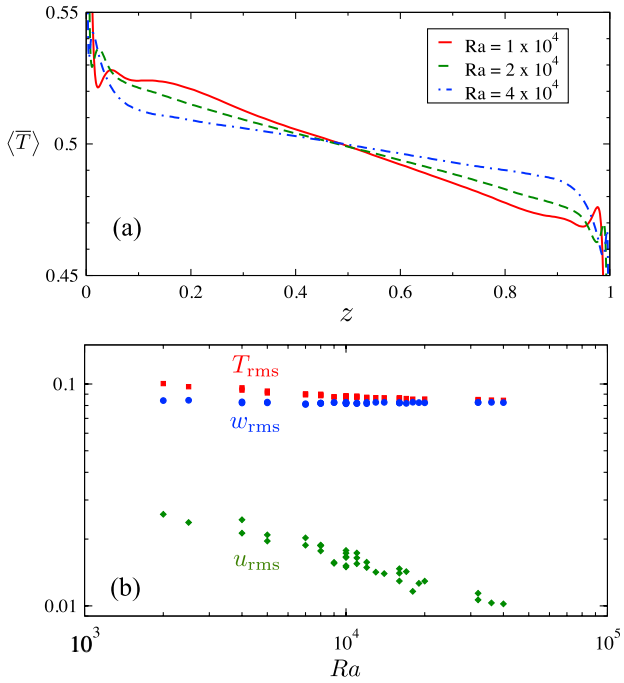

FIG. 3 (color online). Measurements of the interior region: (a) temporally and horizontally averaged temperature profile $\langle \bar{T} \rangle$ for $\mathrm{Ra} = 1, 2, 4 \times 10^4$, and (b) time-averaged root-mean-square values, T_{rms}, u_{rms}, and w_{rms}, of the temperature perturbations and velocity components at $z = 0.5$.

The heat-exchanger model *per se* leaves the wave number k of the columnar flow undetermined. We measured k using a time-average of the Fourier transform of the temperature field at $z = 0.5$, and these measurements are presented in Fig. 4. We obtained very similar results both by applying the same method to the vertical velocity field, and by counting plumes directly using local velocity maxima. The measurements of k can be fitted by an approximate scaling $k \sim \mathrm{Ra}^{0.4}$, though the data also hint at a possible decrease in the exponent for $\mathrm{Ra} > 20\,000$ [19]. There is some variation between different calculations, even for the same aspect ratio L, due to fluctuations in the dominant wave number over extremely long time scales.

A plausible hypothesis is that the horizontal wave number k and the amplitude $\hat{T}$ of the interior columnar exchange flow are determined by the interaction between the megaplumes and the protoplume regions at the top and bottom of the flow. To examine the dynamics in these regions, we constructed space-time diagrams of the temperature in a slice at a fixed height just above the bottom boundary layer, which exhibits behavior that is mirrored at the top. Figure 5 reveals a characteristic repeating "fish-bone" pattern, which corresponds to persistent megaplume roots (the "backbones") together with transient formation and entrainment of protoplumes on either side (the "ribs").

The pattern of ribs shows bursts of protoplumes that typically commence near a larger established plume, while later protoplumes in the burst originate successively further away. We interpret this as propagation of instability along the boundary layer which drains the buoyancy accumulated since the previous burst. Concomitantly each new protoplume is entrained back towards the larger established plume. This coupled mechanism of instability and entrainment leads to episodic and highly time-dependent patterns of plume growth and flushing.

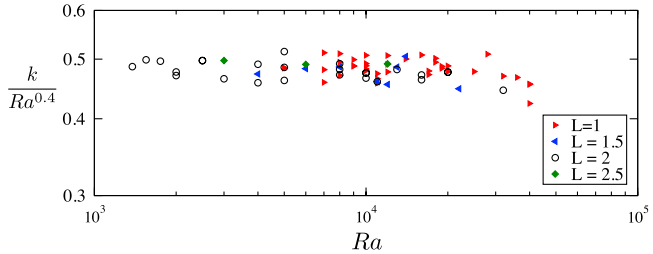

FIG. 4 (color online). Time-averaged horizontal wave number k scaled by $\mathrm{Ra}^{0.4}$, measured from the Fourier spectrum at $z = 0.5$. We attribute the variability in these measurements to very long-time-scale fluctuations in the dominant wave number that are not fully time averaged.

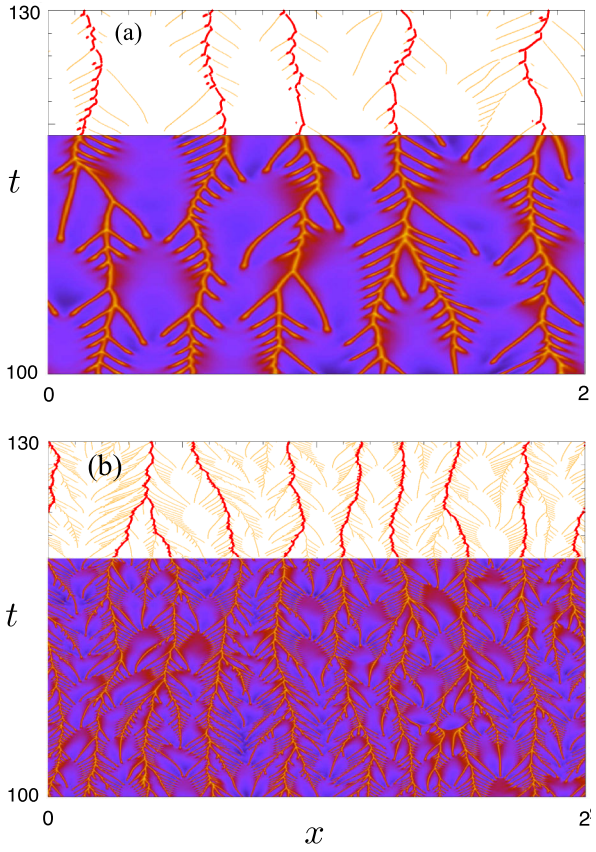

FIG. 5 (color online). Space-time plots of the temperature in a slice just above the boundary layer, for (a) $\mathrm{Ra} = 5 \times 10^3$ at $z = 2 \times 10^{-2}$, and (b) $\mathrm{Ra} = 2 \times 10^4$ at $z = 5 \times 10^{-3}$. These plots show both the directly measured temperature ($t < 120$) and the results of a plume-tracking algorithm ($t > 120$), which gives a way to analyze the dynamics of plumes in more detail. Megaplume roots are highlighted, and the "ribs" of the fish-bone structures (see the text) mark the formation and entrainment of protoplumes.

Comparison of plots like Fig. 5 and counts of protoplumes both suggest that typical time scales and lateral length scales of the "ribs" in the fish-bone structures scale approximately like Ra^{-1} [20]. The length scales certainly decrease significantly more rapidly with Ra than the megaplume spacing k^{-1}, as can be seen by comparing the number of "ribs" in Fig. 5. The difference between the scaling of the protoplumes and megaplumes suggests that the horizontal wave number k of the interior flow is not directly governed by the dynamics of protoplumes at the top and bottom of the domain. We are currently investigating an alternative possibility that k is determined by the stability of the interior columnar flow.

Given the increasingly vigorous nature of the dynamics at the boundaries, it is striking that the interior columnar flow displays such persistent regular structure as Ra increases. Moreover, despite highly time-dependent forcing from the protoplume regions, we have shown that the *steady* heat-exchanger solution provides a remarkably good description of the dynamics of the interior region. It is intriguing that the protoplumes do not appear to govern the interior wave number k directly. These surprising observations, together with our measurements of the flux, have implications for a wide range of buoyancy-driven flows in porous media, including the long-term stabilization of sequestered CO_2 through dissolution-driven convection.

D. R. H. is supported by a studentship from the EPSRC. J. A. N. is grateful for support from the Royal Society through a University Research Fellowship.

[1] M. Cross and P. Hohenberg, Rev. Mod. Phys. **65**, 851 (1993).
[2] L. Kadanoff, Phys. Today **54**, No. 8, 34 (2001).
[3] G. Ahlers, S. Grossmann, and D. Lohse, Rev. Mod. Phys. **81**, 503 (2009).
[4] S. Grossmann and D. Lohse, Phys. Fluids **23**, 045108 (2011).
[5] X. He, D. Funfschilling, H. Nobach, E. Bodenschatz, and G. Ahlers, Phys. Rev. Lett. **108**, 024502 (2012).
[6] H. Hassenzadeh, M. Pooladi-Darvish, and D. Keith, AIChE J. **53**, 1121 (2007).
[7] F. Orr, Jr., Science **325**, 1656 (2009).
[8] S. Kimura, G. Schubert, and J. Strauss, J. Fluid Mech. **166**, 305 (1986).
[9] M. Graham and P. Steen, J. Fluid Mech. **272**, 67 (1994).
[10] J. Otero, L. Dontcheva, H. Johnston, R. Worthing, A. Kurganov, G. Petrova, and C. Doering, J. Fluid Mech. **500**, 263 (2004).
[11] L. Howard, in *Applied Mechanics, Proceedings of the 11th International Congress of Applied Mechanics*, edited by H. Görtler (Springer, Berlin, 1964), pp. 1109–1115.
[12] C. Doering and P. Constantin, J. Fluid Mech. **376**, 263 (1998).
[13] B. Wen, N. Dianati, E. Lunasin, G. Chini, and C. Doering, Commun. Nonlinear Sci. Numer. Simul. **17**, 2191 (2012).
[14] J. Neufeld, M. Hesse, A. Riaz, M. Hallworth, H. Tchelepi, and H. Huppert, Geophys. Res. Lett. **37**, 22404 (2010).
[15] S. Backhaus, K. Turitsyn, and R. Ecke, Phys. Rev. Lett. **106**, 104501(2011).
[16] See Supplemental Material at http://link.aps.org/supplemental/10.1103/PhysRevLett.108.224503 for additional notes on the numerical method.
[17] The dynamics at lower Ra exhibit hysteresis [9,10], but we find that the high-Ra regime is always attained for $\mathrm{Ra} > 1300$.
[18] See Supplemental Material at http://link.aps.org/supplemental/10.1103/PhysRevLett.108.224503 for a movie of the temperature field at $\mathrm{Ra} = 2 \times 10^4$.
[19] A larger range of Ra would be required to verify any change in exponent. However, results from stability analysis of the heat-exchanger solution (not presented here) suggest an asymptotic scaling of $k \sim \mathrm{Ra}^{1/3}$.
[20] Counts from a plume-tracking algorithm suggest a scaling exponent of -0.96 ± 0.05 for the rib spacing.